Zeitschrift: Helvetica Physica Acta
Band: 58 (1985)
Heft: 1

Artikel: Nuclear magnetic resonance studies in solid electrolytes
Autor: Brinkmann, D.
DOI: https://doi.org/10.5169/seals-115586

Helvetica Physica Acta
Vol. 58, 1985 167-182

0018-0238/85/010167-16$1.50+0.20/0

NUCLEAR MAGNETIC RESONANCE STUDIES IN SOLID ELECTROLYTES

D. Brinkmann

Physik-Institut, University of Zurich, 8001 Zurich

By discussing the representative solid electrolytes $RbAg_4I_5$, KAg_4I_5, $LiAlSiO_4$ (eucryptite), and Li_3N it is demonstrated how NMR studies of relaxation, line splitting and shifts, diffusion constants etc. yield information on many aspects of the fast ion transport such as diffusion pathways, hopping times and their activation energies, correlation and dimensionally restricted diffusion, phase transitions etc.

Introduction

Solid electrolytes or superionic conductors as they are sometimes termed, are solid state systems whose ionic conductivities approach values of $10^2(\Omega m)^{-1}$ that are typical of those found in liquid electrolytes. This class of new materials has therefore received large attention for its technological application as solid state batteries, fuel cells, memory devices, display panels etc.

The liquidlike diffusion accompanied by a low activation energy (about 0.1 to 0.5 eV) are the features that distinguish solid electrolytes from "normal" ionic conductors such as NaCl whose ionic conductivity at 200°C is about $10^{-6}(\Omega\ m)^{-1}$. Thus, many researchers in the field consider the superionic state as quantitatively rather than qualitatively different from the normal state. Nevertheless, the high conductivity of the solid electrolytes results from properties usually not met with in other solids: a large number of ions is highly mobile, a network of pathways for the diffusing ions exists, a large degree of disorder is present, and the many-particle aspect of the ionic transport is very important. However, a general theory of the fast ionic transport comprising all superionic solids does not exist at the moment and is not in sight.

For details on theoretical concepts and experimental techniques that deal with the basic rather than with the technological aspects of fast ion transport in solids we refer to the reference list. Ref. [1] to [4] offer reviews of both experimental techniques and theories, [5] is an introductory text, [6] and [7] are concerned with current theoretical concepts.Numerous papers, of course, have appeared in the Proceedings of recent international conferences on fast ion transport [8-10].

Beside those classical techniques like conductivity and tracer diffusion measurements, x-ray and neutron experiments, nuclear magnetic resonance (NMR) has participated in the investigation of superionic conductors right from the beginning of this new research field. These activities are well documented in several review books and articles [11,5,12,13,14,15]. In this paper we will review NMR investigations in some representative solid electrolytes to demonstrate how NMR is able to provide information on the following properties: Type of the diffusing ions, discrimination of different types of motion, hopping rate and activation energy of the diffusing ions, self-diffusion coefficient of the mobile species, dimensionally restricted motion, collective movements. We will discuss the compounds $RbAg_4I_5$, KAg_4I_5, β-$LiAlSiO_4$ (eucryptite), and Li_3N.

$RbAg_4I_5$ and KAg_4I_5

The isostructural compounds MAg_4I_5 (M = Rb, K, or NH_4) represent model systems for the study of superionic solids since they undergo two successive phase transitions at temperatures T_{c1} (around 200 K) and T_{c2} (around 130 K). The transition at T_{c1} occurs within the superionic state of conduction separating the cubic high-temperature α-phase from the rhombohedral medium-temperature β-phase; the trigonal γ-phase is low-conducting [1]. The high conductivity arises at least partly from the fact that the number of Ag sites exceeds the number of mobile Ag ions: In α-$RbAg_4I_5$ there are 16 ions distributed over 56 sites. With decreasing temperature, the structural phase transitions are accompanied by an increase of the order in the Ag distribution.

A first question NMR is able to answer concerns the order of the phase transition. The structural change at T_{c1} has been examined by measuring the positions of the central lines of the ^{87}Rb quadrupole splitting (for a spin 3/2) in $RbAg_4I_5$ [16]. Lines which are present in the α-phase vanish in

the β-phase and are replaced by new lines. If the structural transition were of second order as has been reported in the literature, a continuous change of the electric field gradient (EFG) at the Rb sites and thus a continuous broadening followed by a splitting of these lines should be observed. However, no such effects were detected, lines just appear and disappear in a reproducible manner. Thus, the transition at T_{c1} is of first order. This conclusion is in accord with recent neutron studies [17].

In a similar way the splitting of the ^{87}Rb spectrum may be used as a probe to explore the temperature-pressure phase diagram. The appearance of a new line in the spectrum indicates a transition into a phase of lower symmetry. In this way in $RbAg_4I_5$ a new phase called δ-phase was discovered [18] which exists depending on temperature at pressures beyond 5.7 kbar. This phase is probably low conducting as we will see later.

The main activity of the NMR investigations in $RbAg_4I_5$ and KAg_4I_5 was devoted to the dynamics of the ionic conduction by measuring the spin-lattice relaxation rate $1/T_1$ of both the mobile Ag and the stationary Rb (or K) ions. The time dependent part of the EFG due to the diffusive motion of Ag ions (and perhaps other dynamic properties of the crystal) gives rise to the quadrupolar relaxation of ^{87}Rb. The ^{107}Ag and ^{109}Ag nuclei (both with spin 1/2) relax by means of magnetic interactions. Both relaxation rates can be analyzed in terms of the Bloembergen-Purcell-Pound (BPP)-type formula

$$1/T_1 = C^2\nu/(\nu^2 + \omega^2)$$

where C is a measure for the amplitude of the fluctuating fields, ω is the Larmor frequency, and $\nu = \nu_o \exp(-E/kT)$ is the thermally activated jump frequency of the diffusing Ag ions.

Fig. 1a shows the temperature dependence of the ^{87}Rb relaxation rate for different magnetic fields and crystal orientations [16]. As required by NMR theory two relaxation rates $1/T_1'$ and $1/T_1''$ were observed. Except for the "flat" maxima and the critical behavior above T_{c1}, the data in the α- and β-phase could be fitted by a single BPP type formula:

$$1/T_1' = C^2\nu/(\nu^2 + \omega^2), \quad 1/T_1'' = \frac{4}{3} C^2\nu/(\nu^2 + 4\omega^2)$$

with an activation energy of 0.13 ± 0.01 eV. One may conclude that the Ag diffusion is highly isotropic. The γ- and δ-phase are probably low-conducting

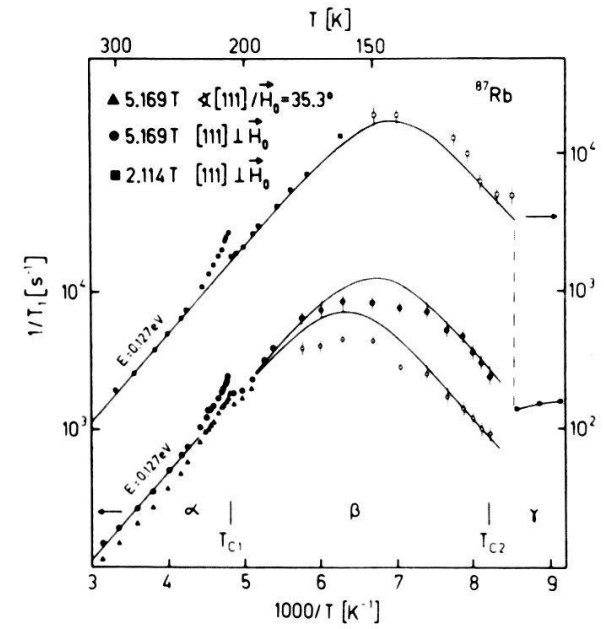

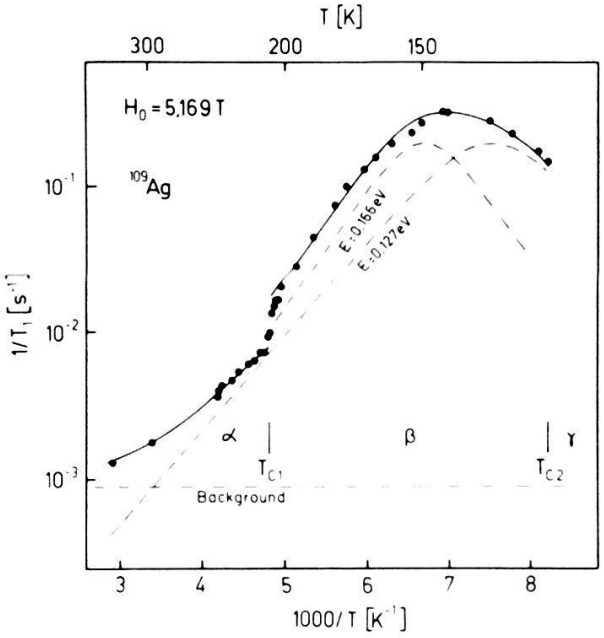

Fig. 1. Temperature dependence of the ^{87}Rb (a) and the ^{109}Ag (b) relaxation rate in $RbAg_4I_5$. The dashed lines in (b) represent the various contributions to $1/T_1$ as described in the text.

since here the Rb relaxation rates are much lower than those of the β- and α-phase.

Fig. 1b shows the temperature dependence of the relaxation rate of ^{109}Ag [16]. The resonance frequency itself exhibits a large chemical shift of - 0.09% with respect to a $AgNO_3$ solution. This suggests that the main relaxation arises from a variation of the anisotropic chemical shift experienced by the moving Ag ion at different sites. A detailed discussion is given in [16] and [19]. The full line in Fig. 1b is the sum of the following contributions: (i) an estimated temperature-independent rate due to paramagnetic impurities ("background"), (ii) BPP-type relaxation with an activation energy 0.13 ± 0.01 eV present in the α- and β-phase due to dipolar interaction with iodine ions, (iii) BPP-type relaxation with an energy of 0.13 eV in the α- and 0.16 eV in the β-phase due to anisotropic chemical shift.

The results are interpreted [16,19] in terms of Funke's "trial and error" model [20]. One assumes that the trial and error hopping of an individual Ag ion is activated with 0.13 eV and is unaffected by the α-β transition. If a hop is successful the surrounding lattice will relax. This configurational response which is activated with 0.17 eV influences the population of the various Ag sites and hence the chemical shift. Thus, the Ag relaxation reflects both the Ag hopping and the lattice response. Tracer diffusion [21] and conductivity [22] measurements, however, yield single activation energies: 0.13 eV for the α- and 0.17 eV for the β-phase.

Further progress in understanding the interdependence of stationary and mobile ions is brought about by measuring the self-diffusion coefficient D_{PMG} of the ^{109}Ag ions by the pulsed magnetic field gradient (PMG) method [23]. The results [24] are plotted in Fig. 2 for the Rb- and K-compound together with tracer data D_T for $RbAg_4I_5$ from Ref. [21]. Here we only want to discuss the results in terms of the Haven ratio $H_R = D_{PMG}/D_\sigma$ [25]. D_σ is defined by the Nernst-Einstein relation $\sigma = (n\, e^2\, D_\sigma)/kT$ where σ is the d.c. conductivity and n is the number of diffusing ions. For 25°C, the literature (see Ref. 24) yields an average value of 25 $(\Omega\ m)^{-1}$. With D_{PMG} (25°C) = 1.8 x 10^{-10} m^2/s from Fig. 2 one obtains $H_R(\alpha) = 0.51$ for the α-phase. Since σ is reduced by a factor 1.07 at the $\alpha \rightarrow \beta$ transition while D_{PMG} decreases by a factor 1.40, the Haven ratio in the β-phase becomes $H_R(\beta) = 0.39$.

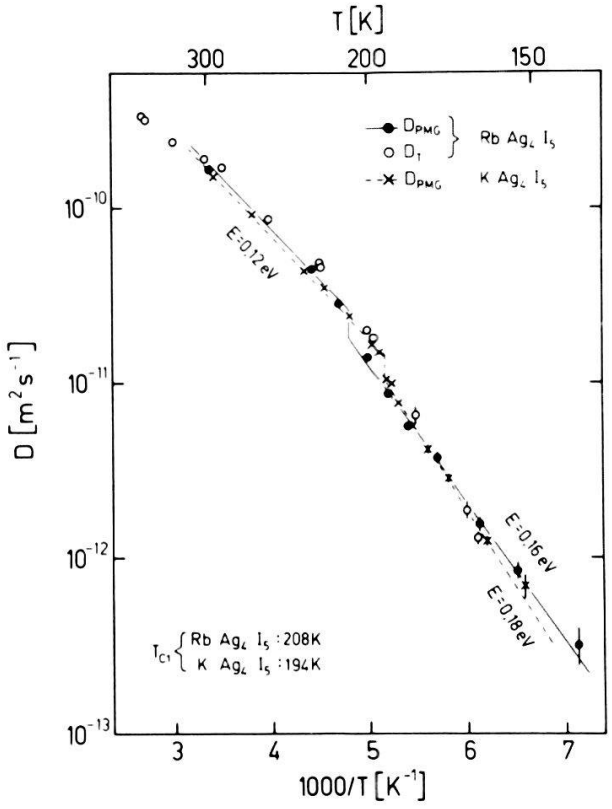

Fig. 2. ^{109}Ag diffusion constants in $RbAg_4I_5$ and KAg_4I_5 determined by NMR (D_{PMG}) and tracer methods (D_T).

These values which are unusually low, may be explained by the"caterpillar" effect [26] which consists in a cooperative motion of two or more ions in such a way that a jumping ion causes other ions to jump in the same direction. The Haven ratio decreases if the number of ions participating in the caterpillar effect increases. One thus may conclude that the correlation of Ag motion in the β-phase is larger than in the α-phase, i.e. the disorder in the Ag distribution has decreased.

$\underline{LiAlSiO_4}$ $\underline{(\beta\text{-eucryptite})}$

In contrast to $RbAg_4I_5$ where diffusion is fairly isotropic, the quartz-like structure of β-eucryptite favors a pronounced one-dimensional (1D) character of ionic conductivity [27]. In the channels along the hexagonal c-axis the Li conductivity is about 10^3 times larger than that in any direction perpendicular to the c-axis. We are now concerned with the question to what

extend NMR parameters such as quadrupolar splittings, linewidths, and relaxation times reflect the 1D properties of β-eucryptite.

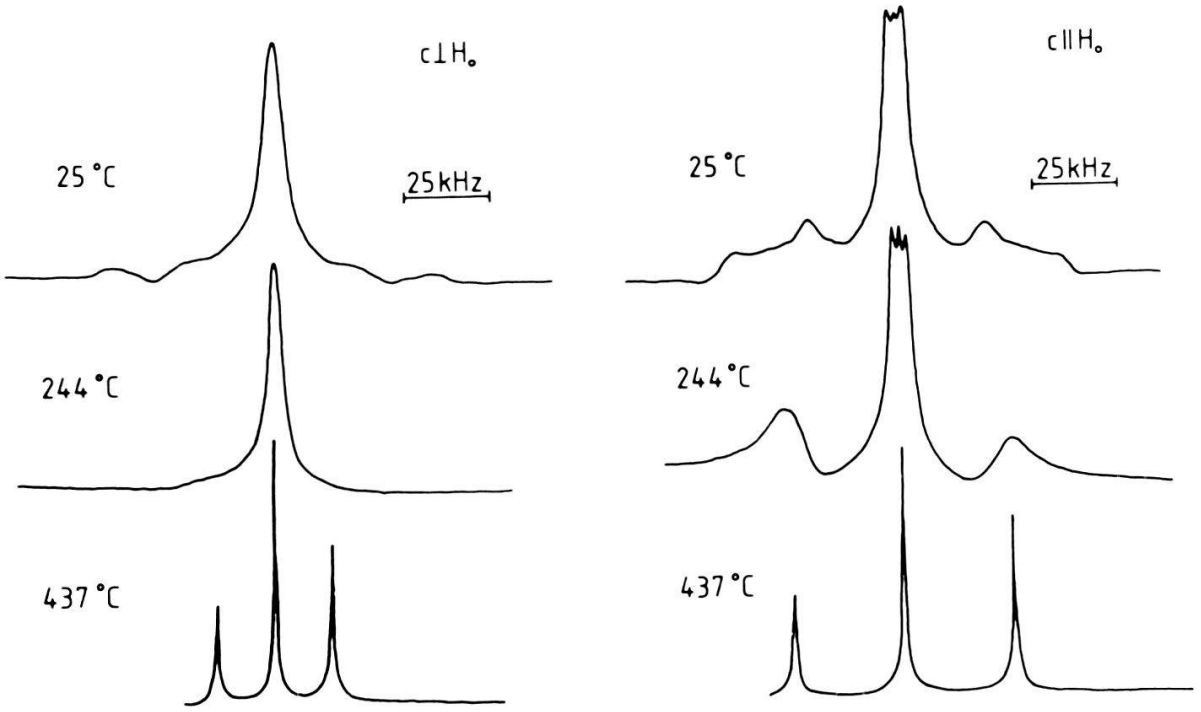

Fig. 3. Temperature dependence of ^{7}Li spectra in $LiAlSiO_4$.

We start with the discussion of the temperature dependence [28] of the spectrum of ^{7}Li (with spin 3/2). Up to about 470 K the spectrum (Fig. 3) represents the superposition of the quadrupolar splittings arising from the three inequivalent Li sites. The EFG tensors at these sites are nearly temperature-independent up to 470 K. Above this temperature the satellites start to merge into a single pair of lines and a single quadrupole splitting results. The corresponding EFG tensor is axially symmetric ($\eta = 0$) with the principal component V_{zz} parallel to the c-axis. This temperature behavior is explained by assuming a Li ion exchange among all inequivalent Li sites thus averaging the EFG's "seen" by individual Li nuclei. The fact that jumps between all inequivalent Li sites are involved in the averaging process could be proved by a careful inspection of the intensity ratio of the satellite and central lines in the averaged spectrum. The theoretical value of 0.75 is verified within 6%. Therefore it was infered that two Li diffusion processes exist: 1D intra-channel diffusion along the main and the secondary channels and inter-channel

diffusion via hopping between different channels.

Despite the presence of these diffusion processes a fine structure of the central signal exists between 100 K and 550 K. It can be shown [29] that this structure arises from a magnetic dipolar coupling of a linear chain of ^{7}Li nuclei moving in a channel with a constant distance between the nuclei. Fig. 4 exhibits the spectrum which has been calculated for the central line assuming a chain of 2, 3 or 4 spins. Dipolar interactions with other spins were taken into account by convoluting each line of the multiplet with a Gaussian function. The most important result is the agreement between the calculated and the measured linewidth. The experimental signal may be interpreted as a superposition of spectra generated by clusters of cooperatively moving Li ions.

The postulated 1D cooperative motion can be checked by measuring the linewidth of the ^{7}Li central signal as a function of temperature. The results are taken from [29] and are given in Fig. 5. For the c-axis parallel to the external field H_o the line narrowing occurs in two steps at 450 K and 550 K; at the "magic angle" only one step (at 450 K) is observed. The narrowing of a linewidth $\Delta\nu$ which arises from dipolar interactions can be related to the correlation time τ of the motion causing the narrowing which is in our case the Li diffusion. In the case of a single process $\Delta\nu$ is given by [30]

$$\Delta\nu^2 = (\Delta\nu)_r^2 + \frac{2}{\pi}(\Delta\nu_{RL,1})^2 \tan^{-1}(2\pi\alpha\tau_1\Delta\nu) \qquad (1)$$

Here, $\Delta\nu_r$ represents the residual linewidth due to interactions not affected by diffusion, $\Delta\nu_{RL}$ is the rigid-lattice linewidth observed in the absence of any motion, and α is a constant of order unity. τ_1 is identified with the mean residence time of the diffusing ions; a thermal activation according to $\tau_1 = \tau_{10}\exp(E_1/kT)$ is assumed. For a two-step process Eq. (1) is replaced by

$$\Delta\nu^2 = \Delta\nu_{r,1}^2 + \frac{2}{\pi}\Delta\nu_{RL,1}^2 \tan^{-1}(2\pi\alpha\tau_1\Delta\nu)$$

where

$$\Delta\nu_{r,1}^2 = \Delta\nu_r^2 + \frac{2}{\pi}\Delta\nu_{RL,2}^2 \tan^{-1}(2\pi\alpha\tau_2\Delta\nu_{r,1})$$

For $c//H_o$ the line narrowing is interpreted as follows. Around 450 K the cooperative motion of the Li ions in a particular channel averages the interaction with Li ions belonging to other channels and the interaction with

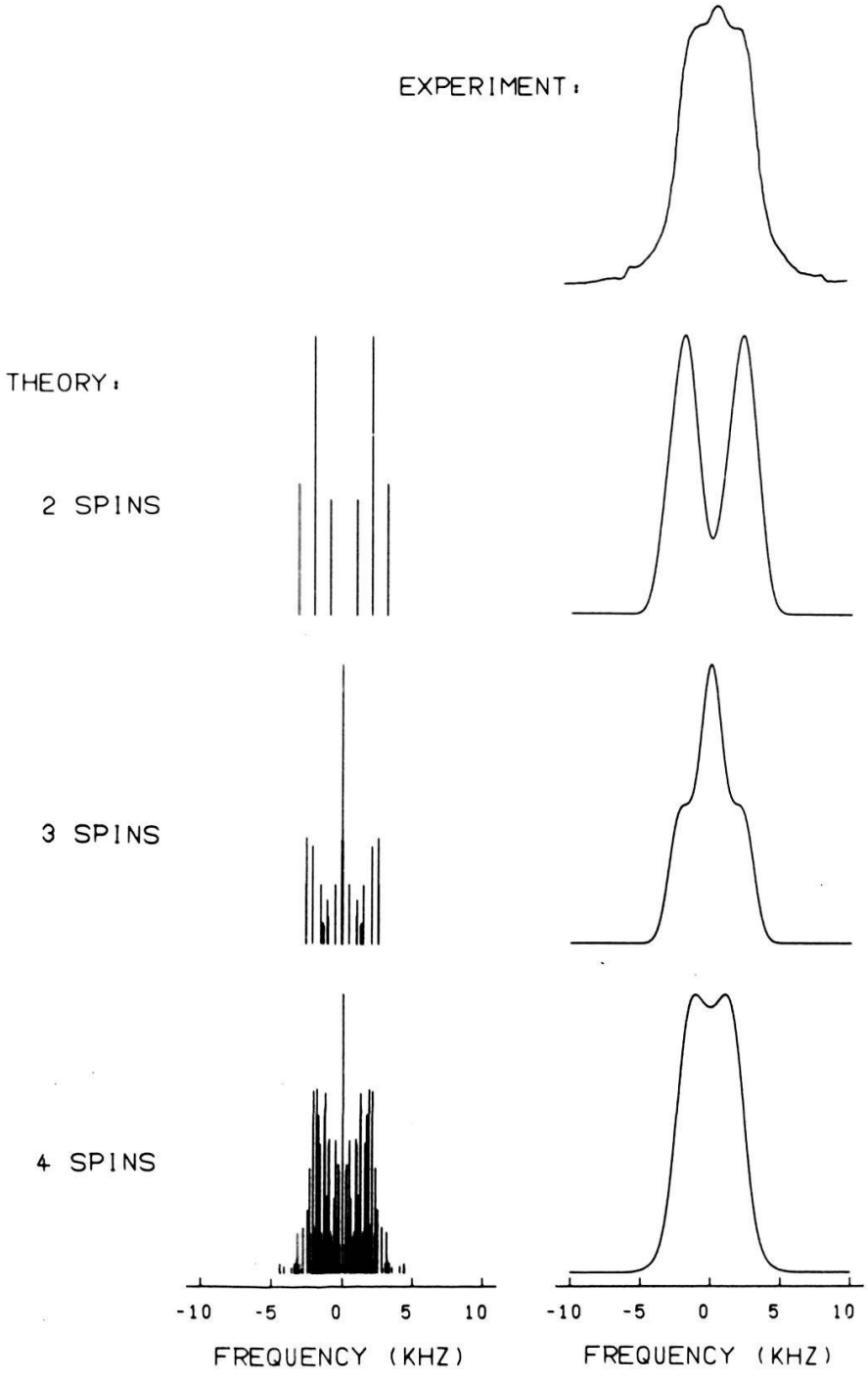

Fig. 4. Experimental and calculated ^{7}Li central signals in $LiAlSiO_4$.

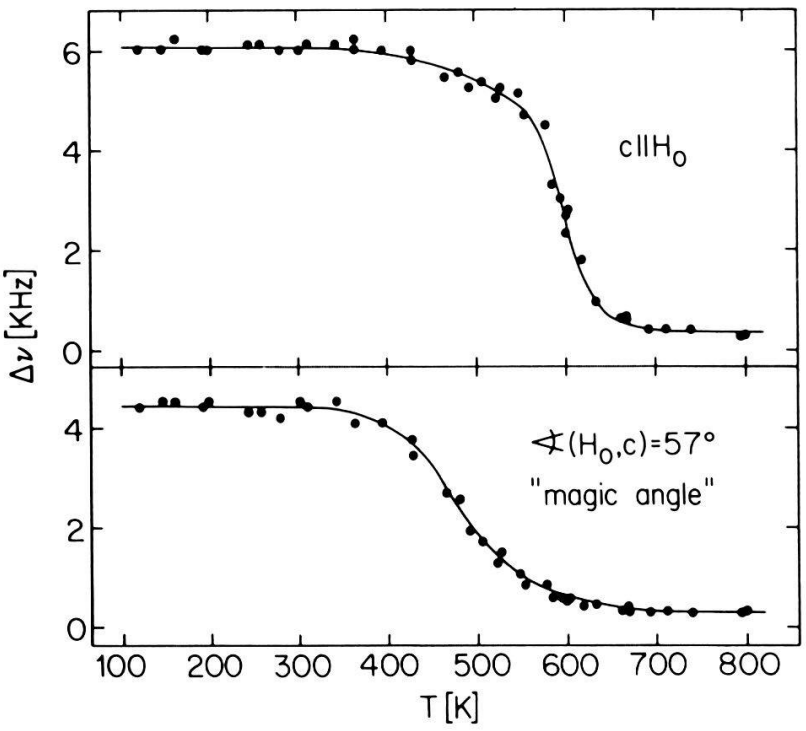

Fig. 5. Temperature dependence of the ^{7}Li linewidth in $LiAlSiO_4$.

Al ions. Then, in a second step the breakdown of the cooperative motion around 550 K averages the interaction between Li ions in the same channel. At the magic angle, however, the dipolar interaction between Li ions of the same channel vanishes and only the averaging of the two other interactions is observed.

The diffusion processes show up also in the relaxation behavior of the ^{7}Li spins. However, due to the presence of paramagnetic ions the analysis and theoretical interpretation is quite involved [29].

$\underline{Li_3N}$

The crystal structure of Li_3N can be considered as a layer structure with alternately Li_2N layers (containing the Li(2) positions) and pure Li layers (with Li(1) positions) perpendicular to the hexagonal c-axis. The Li ionic conductivity is anisotropic with room temperature values $\sigma = 0.001\ (\Omega\ m)^{-1}$ and $\sigma = 0.12\ (\Omega\ m)^{-1}$ parallel and perpendicular to the c-axis, respectively [31]. Conduction is attributed to a vacancy-induced Li diffusion process: the presence of $(NH)^{--}$ and $(NH_2)^{-}$ complexes [32] creates Li

vacancies in the Li_2N layers with a concentration of the order of 1% around 300 K [33].

We will discuss recent NMR investigations in which the resonances of both the stationary ^{14}N nuclei (spin 1) and the mobile ^{6}Li (spin 1) and ^{7}Li (spin 3/2) nuclei were studied. To employ both Li isotopes deepens the insight and allows a double check of many results. All three resonances are split by quadrupole interactions. Based on a point-ion model, the EFG tensors at the two Li sites were calculated [34] and were found to be of the same order of magnitude as the experimental values thus supporting the conclusions that Li_3N is composed of Li^+ and N^{3-} ions [35]. The different signs of the EFG's are in accord with conclusions drawn from the high-temperature behavior of the ^{7}Li quadrupole splitting [36]. Lewis and Schwarzenbach [37] have calculated the EFG's from x-ray data and have refined the parameters of the multipole deformation functions against x-ray and NMR data simultaneously. For the EFG's of Li(1), Li(2), and N they have obtained the sign combination +-- in agreement with the point-ion model.

The ion dynamics were studied by measuring the following NMR observables [36,38]: (i) the second-order quadrupolar shift of the ^{7}Li central signal and its strong temperature dependence between 400 and 600 K (Fig. 6), (ii) the temperature dependence and the extreme angular dependence of the ^{7}Li (Figs. 7 and 8) and ^{6}Li relaxation rates by taking into account different relaxation mechanisms for the two isotopes, (iii) the self-diffusion coefficient of ^{7}Li. The results were interpreted in terms of two diffusion processes: inter-layer diffusion parallel to the c-axis and intra-layer diffusion within the Li_2N layers only.

In the inter-layer diffusion process Li ions of sites (1) and (2) exchange places thus experiencing strongly fluctuating EFG's which cause both spin-lattice relaxation and the temperature-dependent second-order quadrupolar shift. It is assumed that the EFG correlation functions decay exponentially with a correlation time τ which is identified with the mean residence time of the hopping Li ions. To calculate the quadrupolar shift $\Delta\omega^{(2)}$ of the ^{7}Li central signal one starts with an expression derived independently in Ref. [39] and [40]. Then, as shown in [36], this shift is given by

$$\Delta\omega^{(2)} = -\frac{\pi^2}{6\omega}\left(\sin^2\theta\cos^2\theta\,(C_1 + 2C_2)^2\,\frac{1}{1+\omega^2\tau^2}\right.$$
$$+ 3\sin^2\theta\cos^2\theta\,(C_1^2 + 2C_2^2)\frac{\omega^2\tau^2}{1+\omega^2\tau^2} \qquad (2)$$
$$\left. - \frac{1}{8}\sin^4\theta\,(C_1 + 2C_2)^2\,\frac{1}{1+4\omega^2\tau^2} - \frac{3}{8}\sin^4\theta\,(C_1^2 + 2C_2^2)\,\frac{4\omega^2\tau^2}{1+4\omega^2\tau^2}\right)$$

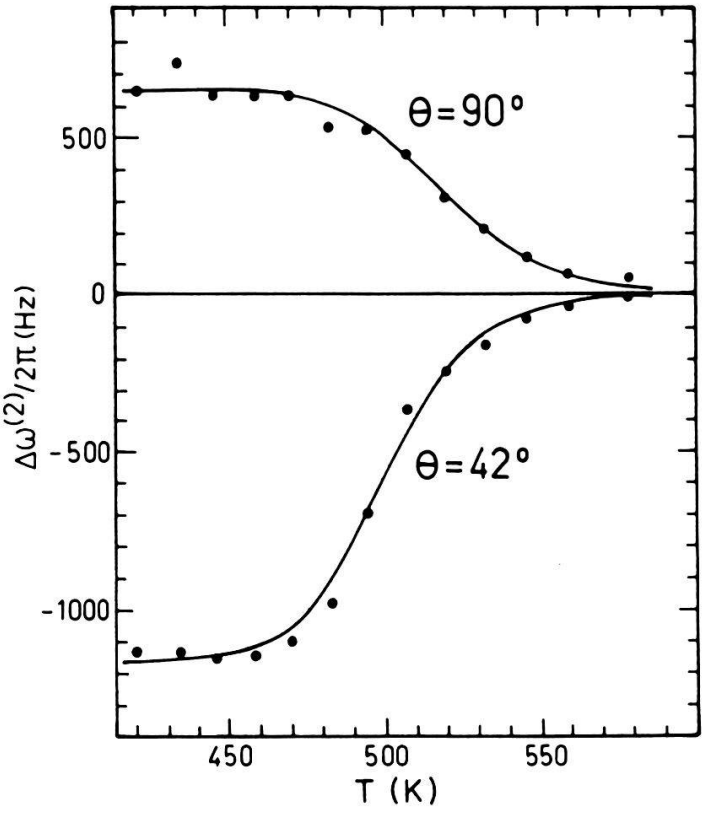

Fig. 6. Second-order quadrupolar shift of ^{7}Li in Li_3N.

Here, θ is the angle between the external magnetic field and the c-axis, and C_1 and C_2 are the quadrupolar coupling constants $C = eQV_{zz}/h$ for the two Li sites where V_{zz} is the principal component of the EFG tensor along the c-axis. By fitting the experimental data of Fig. 6 by Eq. 2 one obtains the jump rate $1/\tau$ which is plotted in Fig. 9.

The spin-lattice relaxation of ^{7}Li caused by the inter-layer diffusion process is given in Fig. 7 by the data points above 420 K. In general, the ^{7}Li 3/2-spin system relaxes by two relaxation rates $R_1 = 2\,W_1$ and $R_2 = 2\,W_2$ where W_1 and W_2 are a measure for the probability of a $\Delta m = 1$ and $\Delta m = 2$ transition, respectively. The calculation based on the ion exchange

process yields [41]

$$W_1 = \frac{\pi^2}{2I} (C_1 - C_2)^2 \sin^2\theta \cos^2\theta \frac{\tau}{1 + \omega^2\tau^2}$$

$$W_2 = \frac{\pi^2}{8I} (C_1 - C_2)^2 \sin^4\theta \frac{\tau}{1 + 4\omega^2\tau^2}$$

A fit of these equations to the data of Fig. 8 produces a second set of $1/\tau$ values. A third set has been obtained from an analysis of the ^{6}Li spin-lattice relaxation rate [36].

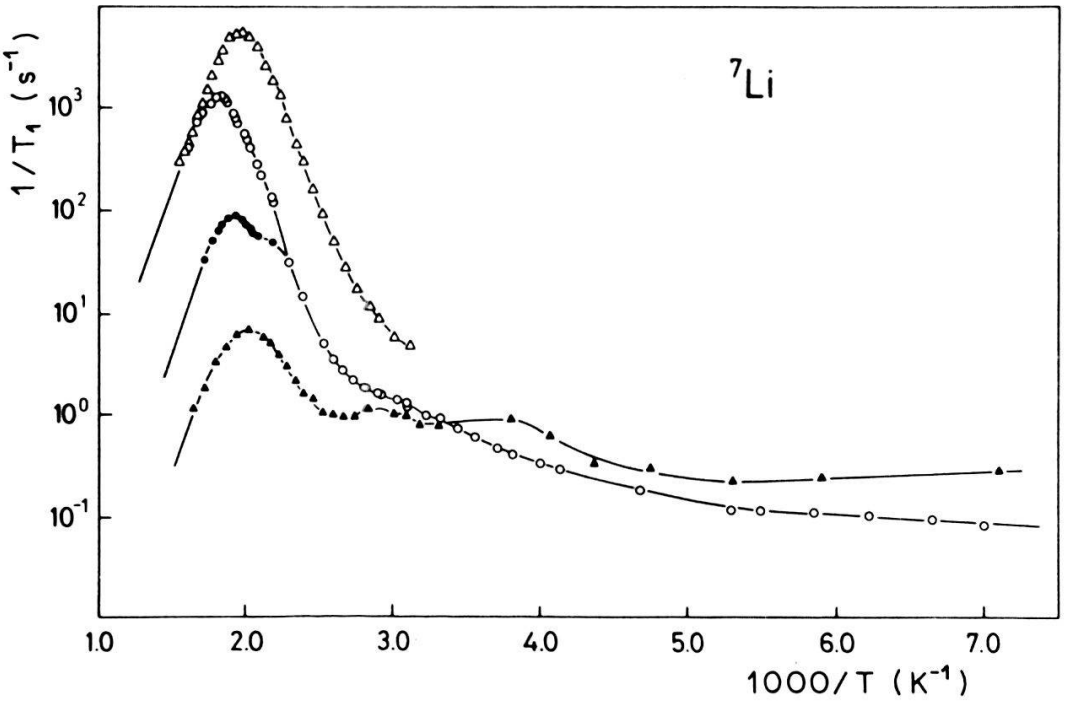

Fig. 7. Relaxation rate of ^{7}Li in Li_3N. $\theta = 90^o$: Δ 8 MHz, ●,○ 34.5 MHz. $\theta = 0^o$: ▲ 34.5 MHz.

Finally, the anisotropic diffusion coefficient of the ^{7}Li nuclei has been measured by the PMG method [38]. By means of the Einstein relation the diffusion data yield the jump rate of the diffusing ions which are also plotted in Fig. 9. One notes good agreement between the jump rates obtained from different sources, in particular, all three sets yield the same activation energy which has also been found in conductivity measurements [32]. Since the shift and relaxation data arise from Li(1) and Li(2) exchanges only, one concludes that these jumps between inequivalent sites are the major contribution

to the diffusion along the c-axis. This contrasts with former x-ray investigations [33] that postulated the dominance of Li(2)-Li(2) jumps. NMR was able to settle this debate.

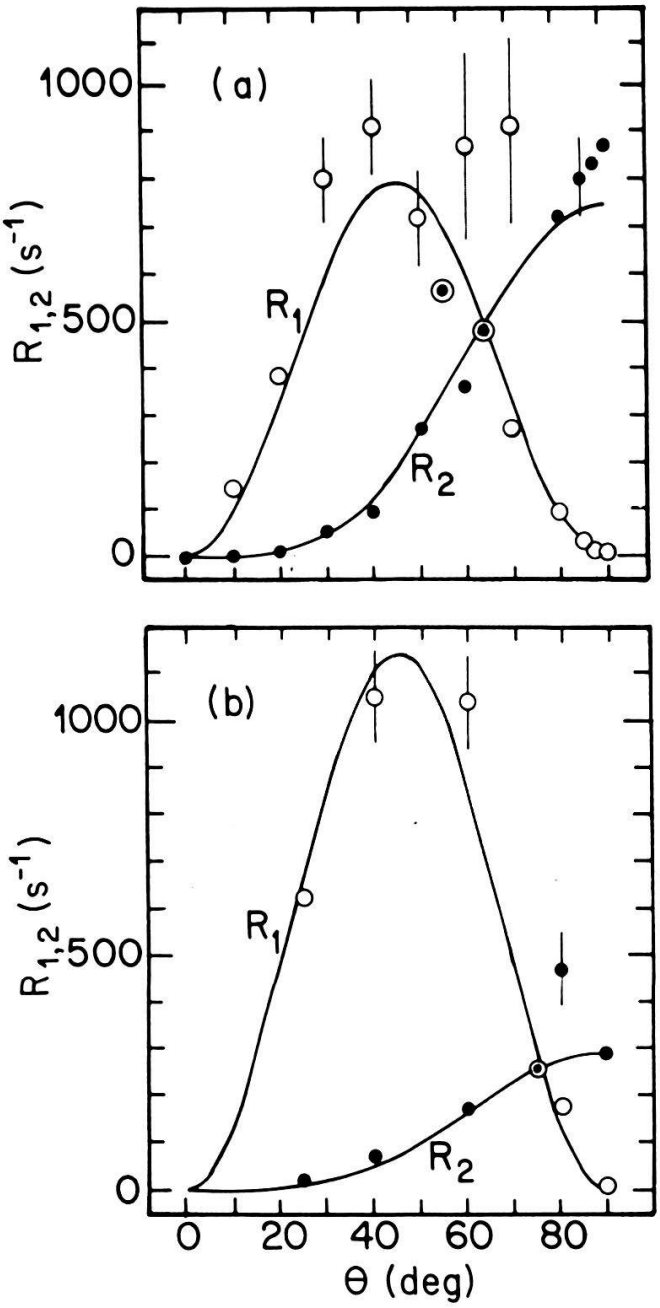

Fig. 8. Angular dependence of ^7Li relaxation rate in Li_3N. (a): T = 593 K, 9.2 MHz, (b): T = 483 K, 35 MHz.

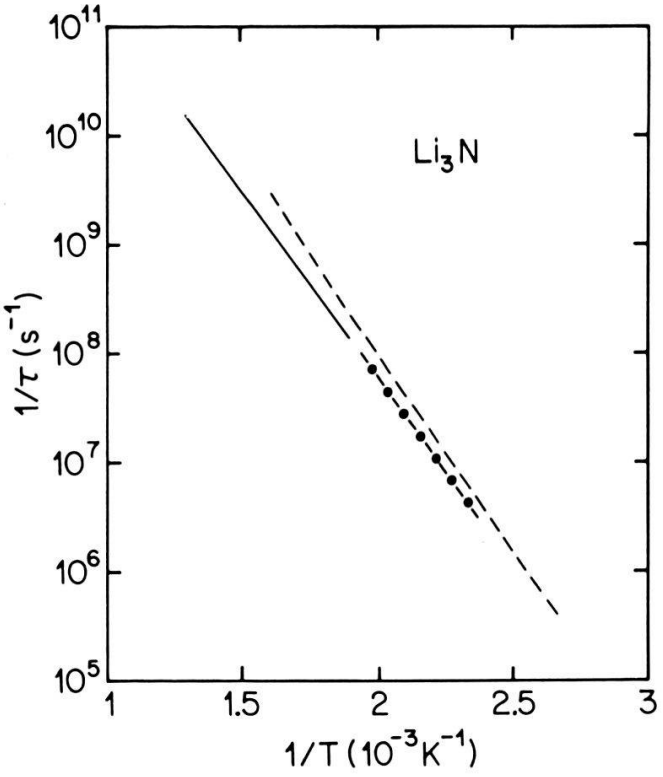

Fig. 9. Temperature dependence of the correlation rate $1/\tau$ of the Li(1)-Li(2) site exchange motion in Li_3N calculated from diffusion (——), second-order quadrupolar shift (-.-.-), and spin-lattice relaxation (---) data of ^7Li.

References

[1] S. Geller, Editor, Solid Electrolytes, Springer-Verlag, Berlin, 1977.
[2] P. Hagenmuller and W. van Gool, Editors, Solid Electrolytes, Academic Press, N.Y., 1978.
[3] M.B. Salamon, Editor, Physics of Superionic Conductors, Topics in Current Physics, Vol. 15, Springer-Verlag, Berlin, 1979.
[4] S. Chandra, Superionic Solids, North-Holland, Amsterdam, 1981.
[5] J.B. Boyce and B.A. Huberman, Phys. Reports 51, 189 (1979).
[6] W. Dieterich, P. Fulde, I. Peschel, Adv. in Physics 29, 527 (1980).
[7] W. Dieterich, in: Festkörperprobleme (Adv. in Solid State Physics), Vol. 21, 325, Vieweg, Braunschweig, 1981.
[8] P. Vashista, J.N. Mundy, G.K. Shenoy, Editors, Fast Ionic Transport in Solids, North-Holland, Amsterdam, 1979.
[9] Proc. Intern. Conf. on Fast Ionic Transport in Solids, Gatlinburg, USA, Solid State Ionics, Vol. 5 (1981).
[10] Proc. Intern. Conf. on Solid State Ionics, Grenoble, France, Solid State Ionics, Vol. 9 & 10 (1983).
[11] P.M. Richards, in Ref. 3.
[12] C. Berthier, in Ref. 8.
[13] J.L. Bjorkstam, M. Villa, Magnetic Resonance Review 6, 1 (1980).

[14] D. Brinkmann, Solid State Ionics 5, 53 (1981).
[15] D. Brinkmann, in: Progress in Solid Electrolytes, T.A. Wheat, A. Ahmad, and A.K. Kuriakose, Editors, Energy, Mines and Resources, Ottawa, Canada, 1983.
[16] H. Looser, D. Brinkmann, M. Mali, J. Roos, Solid State Ionics 5, 485 (1981).
[17] S.M. Shapiro, D. Semmingsen, M. Salamon, Proc. Intern. Conf. on Lattice Dynamics, Flammarion, Paris, 1978.
[18] H. Huber, M. Mali, J. Roos, D. Brinkmann, Rev. Scient. Instr. 55, 1325 (1984).
[19] H. Looser, Dissertation, University of Zurich, 1983.
[20] K. Funke, p. 609 of Ref. 8.
[21] J.S. Arzigian, D. Lazarus, Phys. Rev. B23, 640 (1981).
[22] R.A. Vargas, M.B. Salamon, C.P. Flynn, Phys. Rev. B17, 269 (1977).
[23] E.O. Stejskal, J.E. Tanner, J. of Chem. Phys. 42, 288 (1965).
[24] H. Looser, M. Mali, J. Roos, D. Brinkmann, Solid State Ionics 9 & 10, 1237 (1983).
[25] G.E. Murch, Solid State Ionics 7, 177 (1982).
[26] I. Yokota, J. Phys. Soc. Japan 21, 420 (1966).
[27] U. von Alpen, H. Schulz, G.H. Talat, H. Böhm, Solid State Commun. 23, 911 (1977).
[28] D. Brinkmann, M. Mali, J. Roos, E. Schweickert, Solid State Ionics 5, 433 (1981).
[29] E. Schweickert, M. Mali, J. Roos, D. Brinkmann, P.M. Richards, R.M. Biefeld, Solid State Ionics, 9 & 10, 1317 (1983).
[30] A. Abragam, The Principles of Nuclear Magnetism, Clarendon Press, Oxford, 1961.
[31] U. von Alpen, A. Rabenau, G.H. Talat, Appl.Phys. Lett. 30, 621 (1977).
[32] For instance: J. Wahl, Solid State Commun. 29, 485 (1979).
[33] H. Schulz and K.H. Thiemann, Acta Crystallogr. A35, 309 (1979).
[34] K. Differt and R. Messer, J. Phys. C13, 717 (1980).
[35] K.H. Schwarz and H. Schulz, Acta Crystallogr. A34, 994 (1978).
[36] D. Brinkmann, M. Mali, J. Roos, R. Messer, H. Birli, Phys. Rev. B26, 4810 (1982).
[37] J. Lewis and D.S. Schwarzenbach, Acta Crystallogr. A37, 507 (1981).
[38] E. Bechtold-Schweickert, M. Mali, J. Roos, D. Brinkmann, Phys. Rev. B30, 2891 (1984).
[39] J.L. Bjorkstam and M. Villa, Phys. Rev. B22, 5025 (1980).
[40] L. Schimmele, Ph.D. thesis, University of Stuttgart, Germany (1982).
[41] Taken from [36]; a misprint has been corrected.